Novel polymer nanocomposite hydrogel with natural clay nanotubes

Mingxian Liu, Wendi Li, Jianhua Rong & Changren Zhou

Colloid and Polymer Science
Kolloid-Zeitschrift und Zeitschrift für Polymere

ISSN 0303-402X

Colloid Polym Sci
DOI 10.1007/s00396-012-2588-z

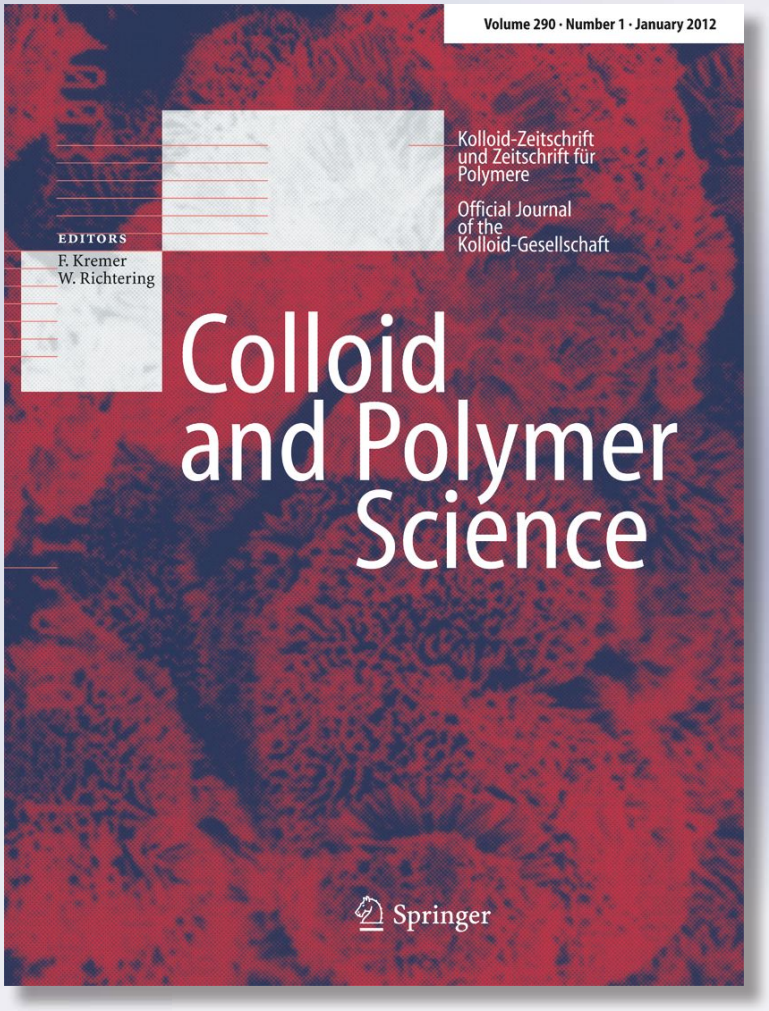

Springer

Colloid Polym Sci (2012) 290:895–905
DOI 10.1007/s00396-012-2588-z

ORIGINAL CONTRIBUTION

Novel polymer nanocomposite hydrogel with natural clay nanotubes

Mingxian Liu · Wendi Li · Jianhua Rong · Changren Zhou

Received: 11 July 2011 / Revised: 3 November 2011 / Accepted: 30 December 2011 / Published online: 17 February 2012

Abstract Polymer nanocomposite gels (NC gels), a kind of typical soft materials, can be synthesized through free-radical polymerization of water-soluble monomers in the presence of nanoclay in aqueous system. Here, novel natural tube-like nanoparticles, halloysite nanotubes (HNTs), are firstly used as multifunctional cross-linkers for polyacrylamide (PAAm) to form a new type of organic/inorganic hybrid hydrogels. Significant improvements in mechanical properties of the PAAm-HNTs NC gels are found by the addition of HNTs as shown by the static mechanical testing and dynamic viscoelasticity measurement. HNTs are uniformly dispersed in the NC gels from the morphological result. HNTs can be intercalated by PAAm chains as observed by the X-ray diffraction result. Hydrogen bonding interactions between HNTs and PAAm are confirmed by the infrared spectroscopy and X-ray photoelectron spectroscopy. The maximum equilibrium degree of swelling (EDS) for the NC gel is 4000% and the EDS decreases with the concentration of clay nanotubes. The present work provides a novel routine for preparing NC gels using "green" one-dimensional nanoparticle. The prepared NC gels have promising application in biomedical areas due to the superior mechanical properties of the gels and good biocompatibility of HNTs.

Keywords Halloysite nanotubes · Hydrogel · Mechanical properties · Nanocomposite

Electronic supplementary material The online version of this article (doi:10.1007/s00396-012-2588-z) contains supplementary material, which is available to authorized users.

M. Liu · W. Li · J. Rong · C. Zhou (✉)
Department of Materials Science and Engineering,
Jinan University,
Guangzhou 510632, China
e-mail: tcrz9@jnu.edu.cn

Introduction

Nanocomposite gels (NC gels) consisting of organic polymer and inorganic nanoparticle was first proposed and fabricated by Haraguchi, a Japanese scientist, in 2002 [1]. The NC gels can be synthesized through in situ free-radical polymerization of water-soluble monomers such as acrylamide and 2-methoxyethylacrylate in the presence of nanoclay in aqueous system, in which the nanoclays act as the multifunctional cross-linking points for the polymer chains [2–4]. Compared with traditional organic cross-linked hydrogel, the NC gels have a unique structure and properties, for example, super optical transparency, ultrahigh tensile extensibility, high swollen ratio and stimuli sensitivities [2]. Therefore, NC gels have been found to be applicable as super-absorbent materials, biomedical materials, smart materials, and so on. A wide range of clay minerals with layered crystal structures, good water swellability, and strong interactions with the water soluble monomers are used as the inorganic component for the NC gels. Typical examples include the smectite-group clays (hectorite, saponite, montmorillonite and so on) and mica-group clays (synthetic fluorine mica). Among these, the artificially synthesized layered silicate "Laponite," with the molecular formula of $[Mg_{5.34}Li_{0.66}Si_8O_{20}(OH)_4]Na_{0.66}$, is mostly used for the preparation of NC gels. Laponite has sufficiently small platelet size (30 nm (diameter)×1 nm (thickness)) and high swelling ability in water (about 35×) for forming clear and colorless colloid dispersion. A series of NC gels have been prepared by combining Laponite with different monomers [1, 4–6]. The ability of forming inorganic/organic hybrid network for NC gels depends on the interactions between the nanoclay and the monomer/polymers, such as, hydrogen bonding and/or ionic interaction. On the other hand, the NC gels cannot be obtained by the polymerization of the

acrylamide monomers with other type of inorganic nanoparticles such as nanosilica or nanotitania [7]. This suggests that the formation of NC gels is highly related to the surface properties and dimensional properties of the nanoparticles. Therefore, further experiments should be done to investigate the effect of nanoparticles on the formation of NC gels. In addition, the viscosity of the Laponite–water systems increases significantly when the concentration of nanoclay is higher than 2 wt.%. For example, the viscosity of the Laponite–water dispersion with 5 wt.% clay content is 1,000 mPa s. As a consequence, it is usually hard to prepare NC gels with high inorganic nanoparticle content using a simple mixing method. By means of a modified procedure or with the aid of surface modification of Laponite, NC gels with high clay content can be obtained [8, 9]. However, these procedures are complicated and energy-consuming. Therefore, exploring other available nanoparticles that can strongly interact with acrylamide or its derivatives for preparation of NC gels with high clay content is generally needed.

Halloysite nanotubes (HNTs) are a kind of naturally deposited aluminosilicate ($Al_2Si_2O_5(OH)_4.nH_2O$), chemically similar to kaolin, which have a predominantly hollow tubular structure in submicrometer range with high aspect ratio [10]. The length of HNTs is about 1 μm, while the inner diameter and the outer diameter of tubes is in the range of 10–30 and 50–70 nm, respectively. The zeta potential of HNTs is mostly negative over a wide pH range due to the surface potential of SiO_2 with a small contribution from the positive Al_2O_3 inner surface [11]. The outer surfaces of HNTs are mainly composed of the Si–O bonds and a few of silanols at the crystal defect sites. In the inner sidewall of HNTs, there are mainly aluminols. Chemical analysis of HNTs reveals a significant amount of metal ions, which arise from the isomorphous substitution for Al^{3+} in the octahedral sheet [10]. The oxygen atoms of Si–O bond at HNTs surfaces are able to form hydrogen bonds with the amide proton of acrylamide, and the metal atoms of the clay may form a complex with the carboxyl oxygen of the monomers. As a result, these features of HNTs render them as possible inorganic components for preparation of NC gels. Also, HNTs are novel nanomaterials for reinforcing polymeric materials. HNTs can be incorporated into different polymers to form nanocomposites via solution mixing or melt mixing [12]. Raw HNTs can be readily dispersed in water by ultrasonic treatment, even with high HNTs concentration (the maximum clay and water ratio in the HNTs water dispersion is nearly 1:1 [weight ratio]). Due to the strong interactions between HNTs and water, with the addition of the small dimensions, no visible sedimentation of HNTs aqueous dispersion occur after stopping ultrasonic treatment for several months if the concentration of HNTs is lower than 10 wt.%. Utilizing the property of good dispersion in water, HNTs can be employed as a carrier for water soluble protective agents or be solution mixed with water-soluble polymers for nanocomposites [13]. For example, polyvinyl alcohol (PVA)/HNTs composite films with high thermal and mechanical properties can be prepared by casting the PVA/HNTs solution [14, 15]. The effects of HNTs on polymers are attributed to the well dispersion of the nanotubes in the polymer matrix and the good interfacial interactions in the systems. Recently, studies on the biocompatibility of HNTs have been conducted to explore their application in biomaterials [15–17]. Vergaro et al. [17] investigated HNTs toxicity and visualized the process of cell uptake of HNTs for different cells. The results demonstrated HNTs' cytocompatibility and potential as a biofriendly cargo nanocontainer for biomaterials. As an alternative one-dimensional nanoparticle for carbon nanotubes, HNTs are cheap, abundantly available, environment friendly, mechanically strong and biocompatible [17, 18]. Therefore, exploring HNTs for NC gel preparation has theoretical and practical significance.

In the present work, HNTs are firstly used as multifunctional cross-linkers of polyacrylamide (PAAm) to form a new type of NC gels. The mechanical, morphological, dynamic viscosity and swelling properties of the PAAm-HNTs NC gels are systematically investigated. The NC gels show dramatic enhancement in mechanical properties both under static and dynamic conditions comparing with linear polymer. These changes of properties are attributed to the uniform dispersion of HNTs and the hydrogen bonding interaction between the nanotubes and PAAm.

In comparison with the well-established Laponite XLG-based NC gels, the PAAm-HNT NC gels is a novel system which combines the advantages of HNTs such as natural, cheap and "green" with the good ability of formation of gel for the acrylamide monomers. The prepared NC gels have a promising application in biomedical areas due to the high mechanical properties and good biocompatibility of HNTs.

Experimental

Materials

Acrylamide (AAm) was purchased from industry and was recrystallized from hexane/toluene mixture. Potassium peroxydisulfate ($K_2S_2O_8$, KPS) was of analytical grade reagent and recrystallized from deionized water. HNTs were mined from Yichang, Hubei, China. The elemental composition was determined by X-ray fluorescence (XRF) as follows (wt.%): SiO_2, 58.91; Al_2O_3, 40.41; Fe_2O_3, 0.275; TiO_2, 0.071. The Brunauer–Emmett–Teller (BET) surface area of the used HNTs was 50.4 m^2/g. HNTs were purified before they were used, according to Shchukin et al. [19]. Pure water was produced by deionization and filtration with a Millipore purification apparatus (resistivity >18.2 MΩ cm)

and bubbled with argon gas for more than 1 h prior to use.

Synthesis of PAAm-HNTs NC gels

NC gels were prepared by in situ free-radical polymerization of AAm in the HNTs aqueous dispersion. The procedure was similar to that reported by Haraguchi and Takehisa [1]. The typical procedure was as follows. First, desired amounts of purified HNTs were dispersed in 20 ml pure water under ultrasonic condition for 1–2 h to ensure a uniform dispersion. Then, 3 g of AAm was added and stirred for 30 min at room temperature. The solutions were bubbled with nitrogen gas for 20 min to replace the oxygen gas in the systems. Finally, 3 ml 20 wt.% KPS solution was added to the system under stirring for 5 min. Then, the mixture solutions were casted into glass tubes with the diameter of 7 or 10 mm. The polymerization was carried out in a vacuum oven at 65 °C for 18 h. The percentage of HNTs used in the text was the weight ratio of HNTs to water. For example, the NC gel with 30% HNTs corresponds to the gel containing 6 g HNTs, 3 g polymer, and 20 g water. The maximum loading of HNTs was 30% in the present work. Further increase of HNTs, the viscosity of the water dispersion of AAm and HNTs increased significantly. As a consequence, it was hard to process the mixture dispersions, such as casting the dispersion to glass tubes. The PAAm linear polymer was also synthesized as a control sample. The preparation method for PAAm linear polymer was similar to that for NC gels, but without HNTs.

Characterization of PAAm-HNTs NC gels

Fourier transform infrared spectroscopy (FTIR)

Dried PAAm and NC gels were obtained by evaporating the water from the corresponding hydrogels under atmosphere condition for at least 7 days. The FTIR spectrum was recorded on a MAGNA-IR760 (Nicolet Co, USA) FTIR spectrometer by conventional KBr pellet method at room temperature. Thirty-two consecutive scans were taken and their average was stored. Spectra were taken from 4,000 to 400 cm^{-1}. The resolution of the wavenumber was 2 cm^{-1}.

X-ray photoelectron spectroscopy (XPS)

XPS spectra of dried and mined PAAm and the NC gel (30% HNTs) were recorded by Kratos Axis Ultra^{DLD}. The spectra of high-resolution survey of the nitrogen and carbon elements were deconvoluted using XPS PEAK 4.1 software into several peaks to compare the variation of the element environment for PAAm before and after interacting with HNTs. All the XPS spectra of the samples were calibrated to the reference graphitic carbon (binding energy [b.e.]= 284.6 eV) [20].

X-ray diffraction (XRD)

XRD profiles were obtained using freeze-dried and milled NC gels samples or HNTs powder using X-ray diffractometer (D8, Bruker Corporation) at room temperature. The scanning angle ranged from 2° to 50°.

Scanning electron microscopy (SEM)

The fractured surfaces of the dried gel sample were plated with a thin layer of gold before the observations. The SEM observations were done using the Philips LEO1530 VP SEM machine. The voltage of the electron beam used for SEM observation was 5 kV.

Determination of mechanical properties

Tensile and compression testing of PAAm-HNTs NC gels were carried out using the Zwick/Roell Z005 machine under 25 °C. The samples for tensile testing were rod samples with diameter of 7 mm and length of 100 mm. The crosshead speed was 100 mm/min. No special treatment was needed to fix the samples, since the gel samples were stuck in the fixture well without slippage in the machine. Since NC gels were generally very soft and could always be elongated extensively, the tensile modulus was obtained using the stress at 100% stain for the tensile testing [3]. The stress–strain curves for elongation–recovery of the NC gels were obtained by stretching the samples to the strain well below the macroscopic rupture strain and reverted at the same speed (100 mm/min). The hysteresis in the stress–strain curve was recorded. The permanent deformation data for NC gels were obtained by comparing the length change of the samples before tensile testing and after 60 min of tensile break. The samples for compression testing were cylinder samples with diameter of 10 mm and thickness of 10 mm. The crosshead speed was 100 mm/min and the compression strength was obtained using the stress at the deformation of 60%. At least five samples for every mechanical property experiments were used to obtained reliable data. Table 1 shows the average of the mechanical property data and the standard derivation, while the curves in Fig. 1 represent the curves of the samples.

Rheological property measurements

Rheological property measurements of linear PAAm and NC gels were conducted with a Kinexus rotational rheometer (Malvern Instruments Ltd) using parallel plates of

Table 1 Mechanical properties value of the NC gels (data in the parentheses are standard deviations)

Samples HNTs (wt.%)	Tensile modulus[a] (kPa)	Tensile strength (kPa)	Elongation at break (%)	Permanent Deformation[b] (%)	Compression Strength[c] (kPa)
5.0	5.1 (0.1)	14.2 (2.3)	379 (30)	0.20(0.05)	42.8 (0.4)
10.0	7.7 (0.1)	25.3 (1.8)	645 (8)	0.16(0.03)	45.3 (0.7)
20.0	8.8 (0.2)	44.8 (2.0)	872 (20)	0.19(0.07)	46.7 (0.9)
30.0	8.6 (0.2)	49.0 (4.2)	1034 (106)	0.22(0.08)	47.7 (0.3)

[a] The tensile modulus was obtained using the stress at 100% stain for the tensile testing

[b] The permanent deformation was obtained by comparing the length of sample after 60 min for tensile break and the initial length of the sample

[c] The compression strength was obtained using the stress at the deformation of 60% during compressive testing

diameter of 20 mm at 25±0.5 °C. The gap between the two parallel plates was set as 1 mm. First, the dynamic strain sweep from 0.01% to 100% was carried out at an angular frequency of 1 Hz. Then, the frequency sweep was performed over the frequency range of 0.001–100 Hz at the fixed strain of 0.5%.

Swelling experiments

Swelling experiments for all samples were performed at room temperature by immersing the dried NC gels (initial size of 1.0 mm [diameter]×5.0 mm [length]) in excess of pure water at room temperature, and changing the water for several times. The weight change of the swollen gel was recorded with time. The equilibrium percentage degree of swelling (EDS) was calculated by the following equation.

$$\text{EDS}\ (\%) = (W_s - W_d)/W_d \times 100\%$$

where W_s is the weight of the swollen gel and W_d is the weight of the corresponding dried gel.

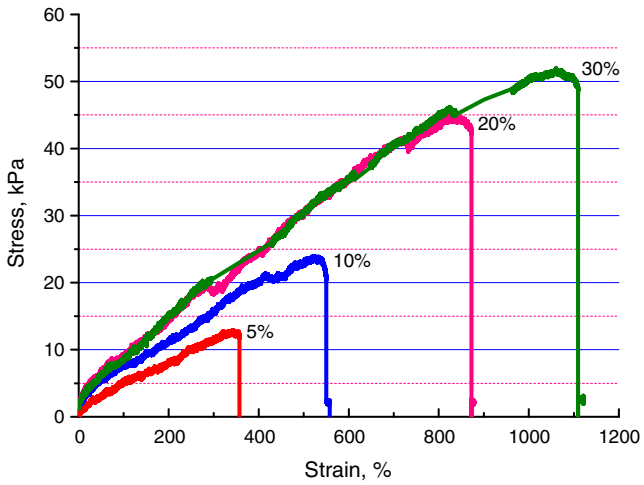

Fig. 1 Tensile stress-strain curves for PAAm-HNTs NC gels

Results and discussion

Mechanical properties of PAAm-HNTs NC gels

NC gels with ultrahigh extensibility and recoverable deformation ability have been recognized since their production in 2002 [1]. Both strength and elongation of the NC gel are superior to those of organic cross-linked gels [2]. To investigate the effect of HNTs on the mechanical performances of PAAm, tensile and compression testing were conducted. Figure 1 shows the tensile stress–strain curves for NC gels. Table 1 summarizes the data of the tensile strength and elongation at break for the NC gels.

One can see that the overall mechanical properties of the NC gels are significantly increased with the loading of HNTs. The increase in tensile modulus, tensile strength and elongation at break of the NC gel is almost proportional to the loading of HNTs. The maximum strength and elongation at break reach 53 kPa and 1,100% for the NC gels with 30% HNTs, respectively. Generally, an increase in strength and modulus for polymeric materials is accompanied by a decrease in elongation at break (ε_b) because the increase is normally caused by the orientation of polymer chains or modification of the polymer structure to a rigid one. However, in NC gels systems, a unique polymer/clay network structure is formed with clay as multi-functional cross-link points [8]. In the present study, HNTs can serve as physical cross-linkers for PAAm chains shown in the following results. Neat PAAm gel is very weak, since there are no cross-linking points. A small amount of HNTs cannot cross-link PAAm molecular chains adequately; therefore, the strength and elongation at break of the NC gels with low HNTs content is low. When the HNT content is increased, HNTs can effectively cross-link the PAAm. As a result, tensile strength and elongation at break of the NC gels increase simultaneously with the HNTs. In Table 1, the tensile modulus of the NC gels is in several kPa, which is comparable with the tensile modulus data in several reports [3, 5]. The modulus increases with HNTs until a loading of 20%. Excess HNTs (30%) tends to slightly decrease the

tensile modulus. This suggests that the cross-linking of the PAAm chains by HNTs reach saturated at the loading of 20% and further inclusion of HNT is just mixed as nanofiller. This will be discussed in detail in the swelling experiment result below.

Figure S1 shows the appearance of the NC gel before, during, and after tensile testing. It can be seen that the NC gel has ultrahigh extensibility and could deform uniformly under tensile force without necking, which is attributed to its low chain density and amorphous structure. The NC gel sample recovers a large proportion of elongation when broken. The stress–strain curves for elongation–recovery of the NC gels are shown in Fig. 2. Nearly no residual strain of the NC gels can be observed for the NC gels. The permanent deformation for all the samples is listed in Table 1. One can see that the permanent deformation after tensile break for all the NC gel samples is less than 1%. This indicates the good elasticity of NC gels. Table 1 also compares the compression strength for NC gels. It also can be seen the compression strength increases with the loading of HNTs. From the mechanical properties results above, it can be concluded that HNTs exhibit an excellent reinforcing effect for the NC gels. This phenomenon is attributed to the high aspect ratio of HNTs and the hydrogen bonding interactions between HNTs and PAAm chains. Upon loading, the stress can transfer from the flexible polymer phase to the rigid inorganic phase via the interfaces. Similar with the poly(N-isopropylacrylamide) (PNIPA)/Laponite systems [2], PAAm chains can be initiated on the surface of HNTs. This can be supported by the sharply increased viscosity of the AAm-HNTs dispersion when incorporating initiator. In contrast, there is no immediate increase of the viscosity for AAm solution when incorporating the initiator. By this mechanism, "clay-brush particles," composed of dispersed

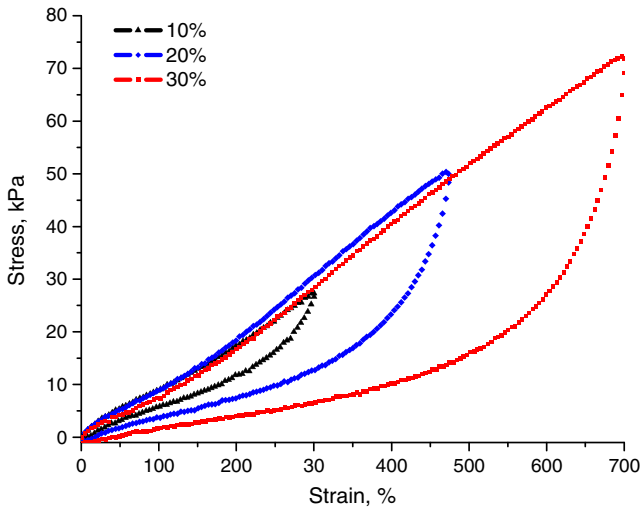

Fig. 2 The stress–strain curves for elongation–recovery of the indicated NC gels

HNTs with numbers of polymer chains grafted to their surfaces, are formed in the NC gel systems. As a result, the PAAm chains can be completely stretched during tensile testing. When unloading the stress, the NC gels can be returned to their initial shape and nearly no permanent deformation is found for the NC gels. This demonstrates that the prepared PAAm-HNTs NC gels are rubber-like materials with good elasticity. The network structure model is shown in Scheme 1. It can be seen that HNTs play the role of physical cross-linking points for PAAm chain. When stretching the NC gels samples, the rolled-up polymer chains that anchored on the HNTs surface can be oriented by the stress. Meanwhile, highly effective loading transfer between nanotubes and the polymer via their interface is responsible for the increased strength. Different from the organic cross-linked hydrogel, the polymer chains which anchored on the HNTs surfaces via physical interactions can be slipping along the tube during the tensile testing. These facts lead to the increased strength and extensibility for the NC gels. It should be pointed that the cross-linking densities for the inorganic nanoparticles cross-linked NC gels systems are much lower than those of covalent bonds cross-linked hydrogel which exhibit fragility [2]. By a layer-by-layer method, ultrastrong and stiff PVA/clay nanocomposites with good interfacial interactions and well distributed nanoplatelets can be obtained [21]. It also should be noted that the values of the mechanical properties for the PAAm-HNTs NC gel is relatively low comparing with those for Laponite XLG-NC gels. For example, the tensile strength and elongation at break of PAAm–Laponite XLG NC gel with 10% clay content is 300 kPa and 1,500%, respectively [5]. The different reinforcing effect of clays arises from the different surface properties and dimensional properties of the nanoparticles. For Laponite XLG, there are numbers of hydroxyl groups on their surfaces, which leads to the strong interactions with the amide side groups of the polymer via hydrogen interactions. The sufficiently small dimension of Laponite makes it much more effective for formation of the polymer/inorganic hybrid network. HNTs also possess numerous hydroxyl groups on their surfaces, so that they can also interact with polymer strongly. But the dimension of the HNTs is much larger than that of Laponite XLG. As a result, with the same clay content, the reinforcing effect of HNTs for NC gels is relatively lower than that of Laponite XLG.

Interactions between PAAm and HNTs

The mechanism of forming NC gels during in situ free-radical polymerization has been proposed according to the changes in viscosity for the designed systems by Haraguchi et al. [7]. The result shows that the initiator (KPS), rather than the monomer, is located near the clay surface through

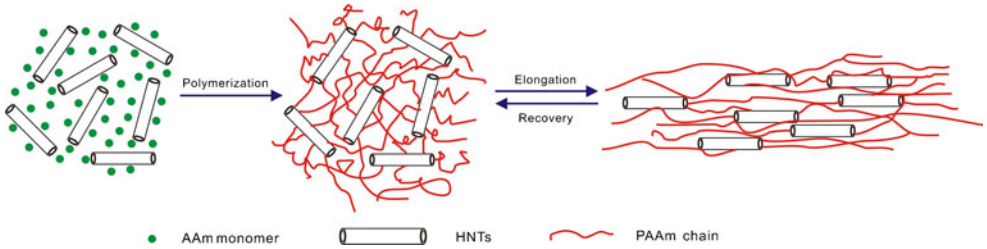

Scheme 1 Schematic representation of the network structure formation and the tensile testing process of the NC gels

ionic interactions. On the other hand, Haraguchi [2] speculated that the interactions between the PAAm and the nanoclay are hydrogen bonds of the amide side groups of the polymer and the surface of the clay (SiOH, Si–O–Si units), but he reported that any difference in FTIR spectra for PNIPA and dried NC gel is found. To illustrate the interactions between PAAm and HNTs, the FTIR and XPS spectra of the PAAm and NC gels were compared. Figure 3 shows the FTIR spectrum of PAAm, dried NC gel, and HNTs. As expected, there are characteristic peaks of both HNTs and PAAm for the dried NC gels. For example, the peaks around 3,620 and 3,695 cm^{-1}, which are assigned to the vibration of inner hydroxyl groups and the hydroxyl groups residing at the octahedral surface of HNTs, respectively [22]. Interestingly, a new peak around 2,782 cm^{-1} appears for the dried NC gels independent of the HNTs content. This peak is ascribed to the confined C–H bond vibration for the PAAm chains [23]. Due to the interfacial interactions between HNTs and PAAm, the arrangement of PAAm chain in the NC gels is significantly restricted by HNTs. Therefore, the configuration of PAAm in NC gels differs from that in pure PAAm. The peak around 1,628 cm^{-1}, which is ascribed to the in plane deformation vibration of N–H bond for the PAAm, shifts to a lower wavenumber for dried NC gels. This is attributed to the presence of the hydrogen bonding interactions between the

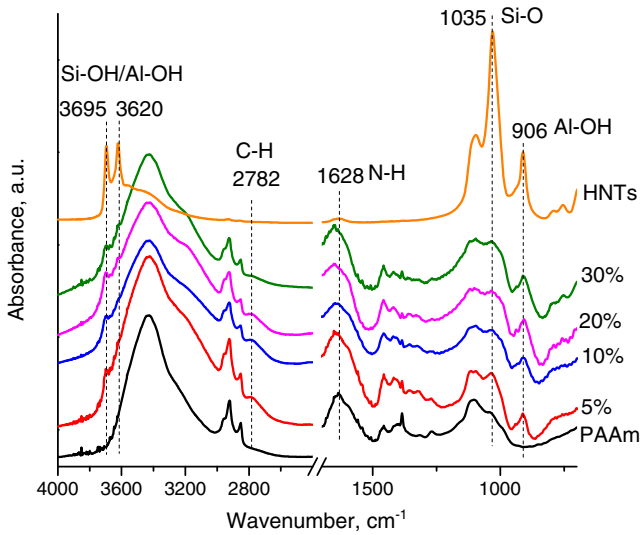

Fig. 3 FTIR spectra of PAAm, HNTs, and dried NC gels

N–H bond of PAAm and Si–O bond of HNTs. The shift of the IR peaks induced by hydrogen bonding interaction has also been found in other systems [24, 25]. The peak around 3,430 cm^{-1}, which is ascribed to the stretching vibration of N–H bond, however, does not shift for all samples. The difference may be attributed to that the sensibility of IR technique for formation of hydrogen bonding of the stretching vibration and the deformation vibration for the N–H bonds are different.

To further substantiate the formation of hydrogen interactions between HNTs and PAAm, an XPS experiment for dried PAAm gel and dried NC gel is conducted. Figure 4a shows the high-resolution XPS spectra of nitrogen atom in the two samples respectively. As shown in Fig. 4a, the binding energy of nitrogen atom for the dried NC gels is decreased to 399.2 eV, while it is 399.7 eV for the PAAm samples. It is considered that the decrease of the binding energy of nitrogen atoms is attributable to the formation of hydrogen interactions between N–H bond in the PAAm chains and Si–O bond as shown in the FTIR results above. Figure 4b and c compares high-resolution XPS spectra of carbon atom in the two samples. It can be seen that the peak for C 1 s can be deconvoluted into three peaks at 284.6, 285.5 and 287.9 eV, which is assigned to the C–H species, C–N species, and O=C–N species of PAAm, respectively [26]. In the dried NC gel sample, the three peaks can also be identified. The change of the strength of O=C–N peak in Fig. 4b and c can be attributed to the formation of hydrogen bonding between the O=C–N bond of PAAm with the silanols and/or aluminols of HNTs. Interestingly, a new peak at 288.4 eV were found, which is assigned to carbon of carbonate-type species at a confined environment of PAAm chains for the dried NC gels because of the interactions between PAAm and the nanotubes [27]. Consequently, the XPS results together with the FTIR results confirm the formation of hydrogen bonding in the NC gel systems.

Viscoelastic properties of PAAm-HNTs NC gels

In theory, enhancements in the rheological properties of polymer materials can be achieved by adding nanofillers due to the high surface area of nanoparticles and the interfacial interactions in the composites. For instance, upon the addition of carbon nanotubes into a polymeric matrix, large increases in the low shear viscosity were observed [28]. The

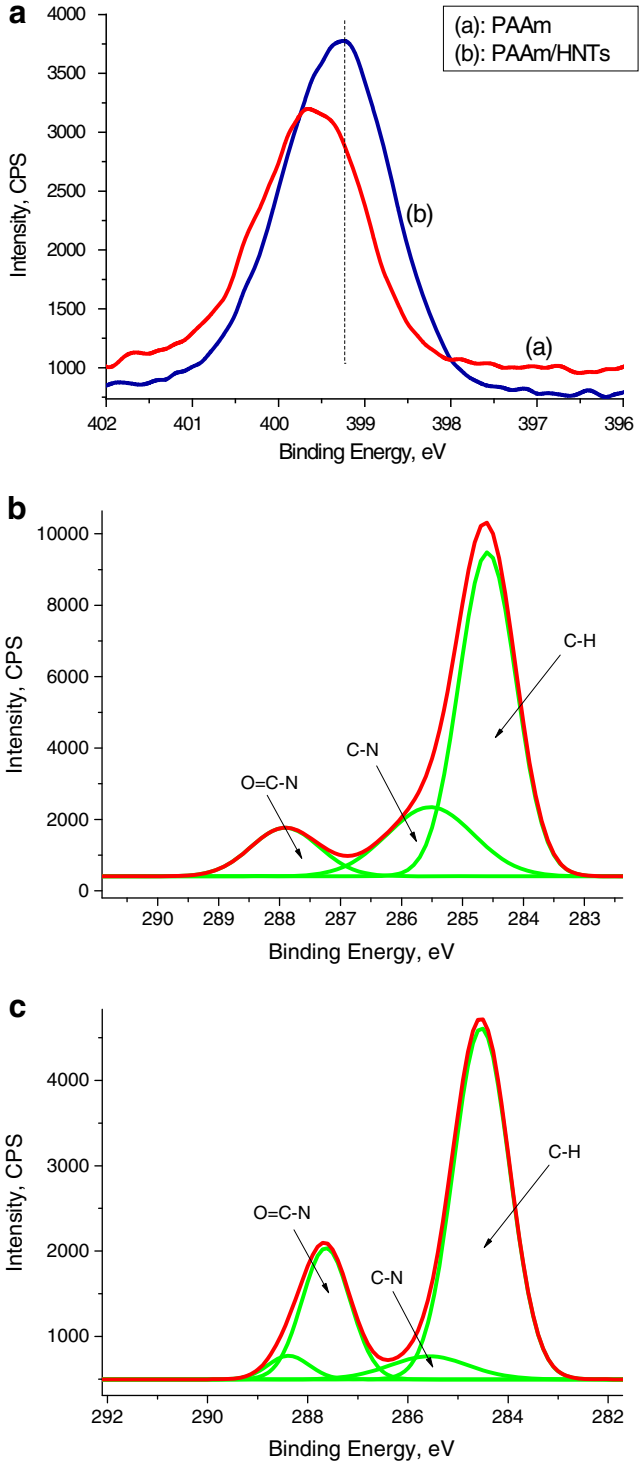

Fig. 4 High-resolution XPS spectra of nitrogen atom (**a**), carbon atom for PAAm (**b**) and carbon atom for the dried NC gels (**c**)

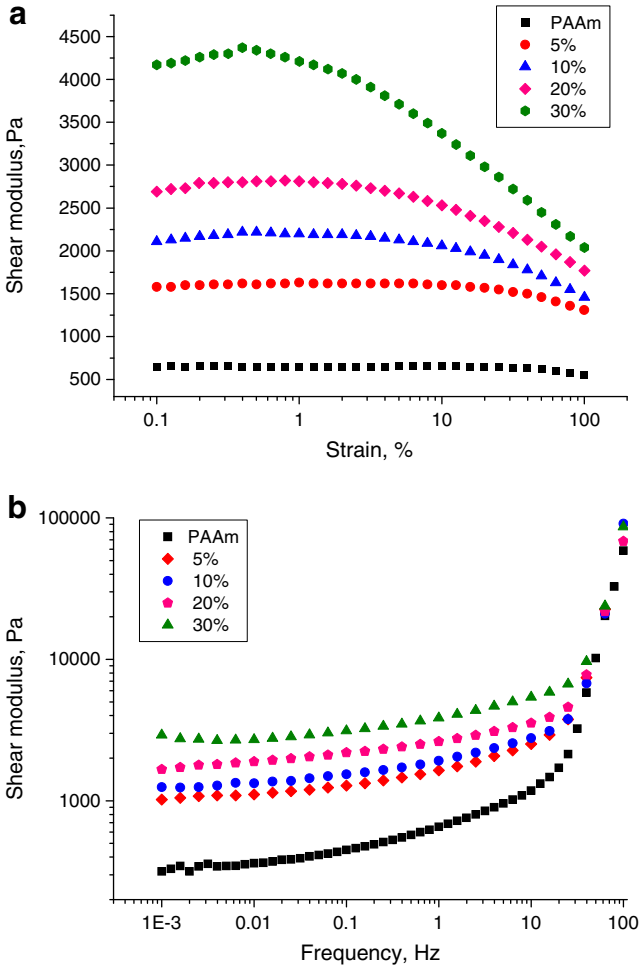

Fig. 5 Strain (**a**) and angular frequency (**b**) dependence of storage modulus G' at 25 °C for PAAm and PAAm-HNTs NC gels

increase was attributed to be the result of the formation of a "gel-like" transient network for carbon nanotube which leads to the increase in mechanical strength. The dynamic viscoelastic properties of PAAm-HNTs NC gels were examined in dynamic stress environment by rheometer. Figure 5a shows the shear modulus (G') curves of the NC gels as a function of strain. The absolute values of the shear modulus for the NC gels substantially increase with the loading of HNTs, in consistent with the change of the mechanical properties shown in Table 1. For example, the G' at 1% strain of NC gels with 30% HNTs is 4,210 Pa, which is 551% and 158% higher than that of the control sample and the NC gel with 5% HNTs, respectively. The value of the shear modulus of linear PAAm is nearly independent of strains over the range from 0.1% to 100%. For NC gels with 30% HNTs, the shear modules sharply decreases with the increasing strain. The difference among the samples may arise from the formation of two types of network structures in the NC gel: the soft but tight polymer network and the rigid but loose inorganic network. The polymer network is formed by the cross-linked PAAm chains via strong hydrogen interactions and entanglement of molecular chains, while the inorganic network is formed via the hydrogen bonds and/or ionic interactions among the tubes (Scheme 1). Upon loading, the relative loose inorganic networks can be seriously destroyed by the

stress. So the shear modulus decreases sharply for the NC gels. The formation of filler networks in the polymer matrix was also found in other systems [29, 30]. Actually, in the Laponite XLG NC gels, the nanoclays can also form so-called "house-of-card" structures through ionic interactions [7].

The frequency sweeping results also demonstrate the reinforcing effect of HNTs on the NC gels. Figure 5b depicts angular frequency dependence of the shear modulus for the NC gels with a comparison of the linear PAAm. Consistent with the mechanical properties results, the G' for NC gels increases with the loading of HNTs at the frequency range of 0.001 to about 20 Hz. The rheological property result is also consistent with previous reported PNIPA–Laponite systems [6]. However, the G' increases sharply for all samples at relative high frequencies, and no difference for these samples can be identified. At high frequencies, only the mobility of bond length and the bond angle can occur for all samples, while the movement of the chain segments cannot take place. As has been discussed above, the addition of HNTs into the NC gels mainly affects the network structures of polymers. Therefore, the effect of HNTs concentration on the shear modulus is much lower at high frequency than that at low frequency. In all, the rheology measurement of the NC gels further suggests the excellent reinforcing effect of HNTs for the NC gels.

Microstructure of PAAm-HNTs NC gels

To understand the mechanical property behaviors of the NC gels, the microstructures of NC gels were analyzed via SEM and XRD methods. The dispersion of HNTs in NC gel was firstly examined by SEM. Figure 6 shows the SEM photos for NC gel with different HNTs content. One can see that the nanotubes can be uniformly distributed in the matrix. No aggregate of the HNTs can be found in any composites. The good dispersion of HNTs is attributed to the proper aspect ratio and relatively weak tube–tube interactions of HNTs [31]. From the SEM photos, it can be seen that the outer walls of HNTs are less distinguished compared to that of raw HNTs, indicating the wrapping of tubes by the grafted PAAm chains. This is attributed to the formation of hydrogen bonding interactions between HNTs and PAAm chains as illustrated by FTIR and XPS results deiscussed above. As suggested by Haraguchi et al., about 1-nm-thick polymer layer is located on the outer surface of nanoclay forming a "clay-brush particle" structure during the polymerization [32]. The uniformly dispersed HNTs and the good interfacial bonding of the NC gels transfer and bear the stress upon loadings [33]. As a result, the hydrogels containing HNTs exhibit unique mechanical properties.

The microstructures of the NC gels were further studied by XRD, and the results are shown in Fig. 7. Since PAAm is amorphous, no diffraction peak of PAAm sample can be observed but a confusion peak appears in the range 10–30°. For the pristine HNTs, the diffraction peak is located around 12.0°, which is associated with to 7 Å (001 plane) of the layer distance of HNTs [10]. After HNTs and PAAm forming NC gels, the diffraction peaks around 12° shift to a lower angle with HNTs loading, which indicates the increase in basal spacing of the HNTs. This phenomenon

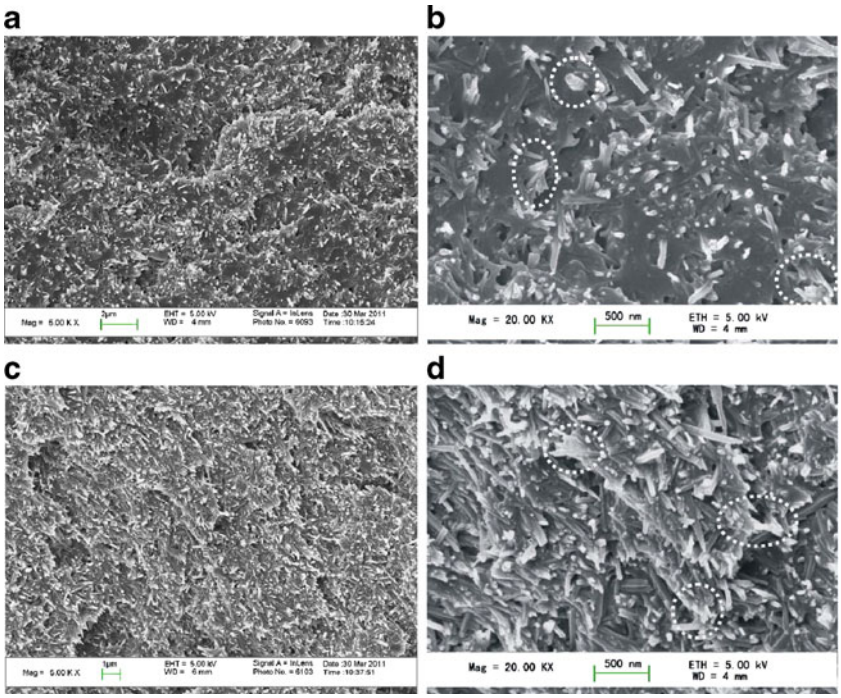

Fig. 6 SEM photos of PAAm-HNTs nanocomposites: **a**, **b** 10% HNTs; **c**, **d** 30% HNTs. (The regions in the white circle represent the tube warped by the polymer matrix)

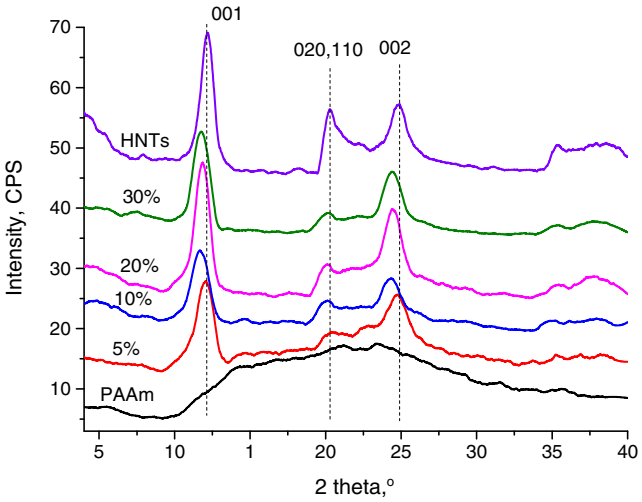

Fig. 7 XRD of PAAm, HNTs and PAAm-HNTs nanocomposites

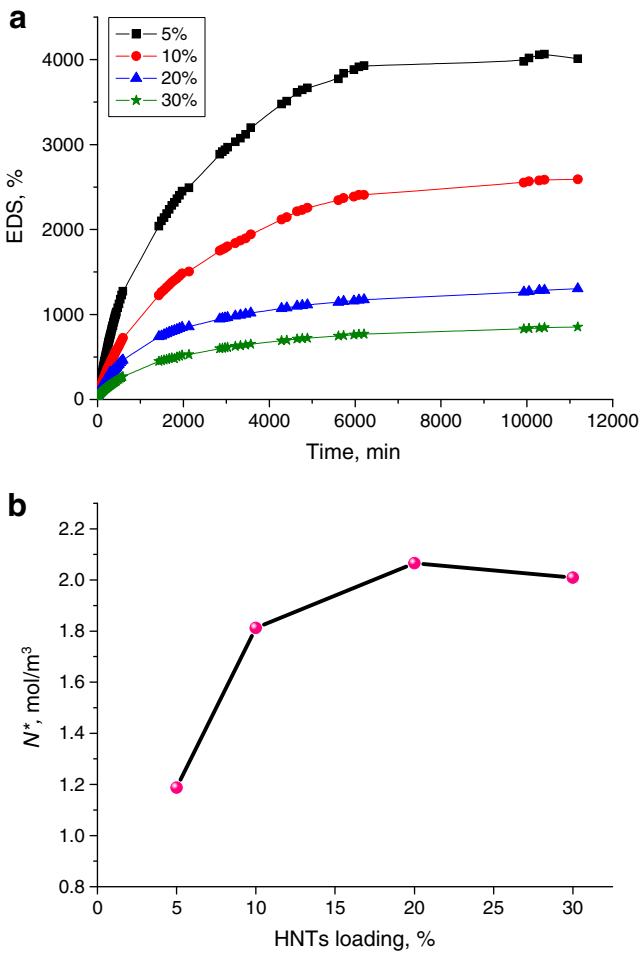

Fig. 8 The equilibrium swelling ratio curves for different NC gel samples as a function of swelling time(**a**) and the effective network chain density (N^*) of NC gels with different HNTs loading (**b**)

suggests that the HNTs can be intercalated by the PAAm molecular chains during the preparation processes of the NC gels. Apart from the change of the peak around 12°, the peaks around 20° and 25°, assigned to 4.4 and 3.5 Å basal reflections of HNTs, respectively, are also changed in the nanocomposites. The intensity of the peak around 20° decreases in all NC gels even with 5% HNTs. The peak around 25° for all NC gels shifts to a lower 2θ value. These phenomena suggest the strong interactions between polymer chains and HNT. The change of the XRD pattern of HNTs is extraordinary in accordance with the results of Rooj et al. [34]. It has been reported that HNTs can also be intercalated by other polymers or compounds [35–37].

Swelling properties of PAAm-HNTs NC gels

NC gels are reported to have high swelling ratio in water, so they can be used as super water absorbent. In the prepared state, NC gels are not fully swollen. To determine their swelling properties, the dried gels were soaked in a large amount of waters. Figure 8a shows the equilibrium swelling ratio curves for different NC gel samples as a function of swelling time. It can be seen that EDS decreases with the loading of HNTs. It is generally considered that the equilibrium swelling ratio of hydrogel depends on the hydrophilicity of the polymer chains and the physical structure. Incorporation of HNTs into the NC gels can result in decrease in the polymer ratio of the NC gels. Since the water sorption of the nanoclay is limited, it is considered that the water sorption property of the NC gels make the main contribution to the water sorption of the polymer networks. As a result, the decreased polymer component in the NC gels results in the decreased EDS. In addition, the increase in HNTs loading in the NC gels leads to the increases in cross-linking density of polymers. The increased cross-link density makes the space among the network for water molecules smaller. A network of gels cross-linked by covalent bonds (OR gels) is dense, inhomogeneous, and unchangeable. As a result, the OR gels have low EDS in water [38]. Due to these effects, the relative water sorption amount decreases with the concentration of HNTs. This result is consistent with the NC gels containing Laoponite [3]. The EDS of NC gel with 5% HNTs is 4,000%, which means that the weight of the swollen NC gels is 40 times more than that of dried gel. The water for swelling all the NC gels is clear, which also supports the formation of inorganic/organic networks via strong interactions between HNTs and PAAm chains. Otherwise, the HNTs should be extracted from the NC gels during the experiment and milk-color HNTs aqueous solutions should be obtained. The appearance of the as-prepared, dried and after swollen for the NC gels is shown in Fig. S2. From the photos, it can be seen that the as-prepared and swelling NC gels are white and opaque. This is different from the Laponite incorporated PAAm or PNIPA hydrogel, which are totally

transparent regardless of the Laponite concentrations. This difference may be caused by the different dimensions of the two types of nanoparticles. As has been discussed above, HNTs are bigger than Laponite in terms of molecular size. The relatively large dimensions of HNTs make the NC gels containing HNTs seem opaque, although the HNTs are uniformly distributed in the NC gels as shown in the SEM photos.

To estimate the network chain density of these samples, the value of N^* are calculated based on the elongation data according to the following equation [3].

$$\tau = N^* RT\left[\alpha - (1/\alpha)^2\right]$$

where τ is the stress at elongation of α=2 (stain 100%), and R and T are the gas constant and absolute temperature, respectively. The N^* values for NC gels are depicted in Fig. 8b. It is can also be seen that the N^* of NC gels increases with the content of HNTs firstly and then the values become steady. The increasing trend of N^* with nanoclay content is consistent with the previous swelling results and the NC gels systems containing Laponite [3, 6]. It seems that a small amount of HNTs (5%) has an insignificant influence on the formation of cross-linking network structure of the NC gels. This can be explained by the fact that a small amount of HNTs cannot completely cross-link the PAAm chains. The mechanical properties, especially the tensile property of NC gels with 5% HNTs, are also relatively low. The effective network chain density (N^*) increases with increasing clay concentration due to an increase in the junction number formed by the nanotubes. When the loading of HNTs is above 20%, it seems that N^* is saturated. This suggests that the small amount (till 20%) of HNTs acts as cross-linker, but further inclusion of HNT is just mixed as nanofiller. The present values of N^* for NC gels is comparable with that of the PNIPA–Laponite XLG NC gels [6].

Conclusions

A novel naturally occurring nanotube, HNTs, are firstly used to prepare NC gels by in situ free radical polymerization of acrylamide monomers. The tensile property, compression strength and shear modulus of the NC gels significantly increase by HNTs. HNTs have a good dispersion state without aggregates in the NC gels, and they can be intercalated by the PAAm chains. This is attributed to the strong interfacial interactions between HNTs and PAAm chains, predominately the hydrogen bonding. The swelling property of NC gels is dependent on the HNT content. The equilibrium swelling ratio of NC gels with 5% HNTs content reaches a maximum of 4,000%. Due to the unique structure and properties of PAAm-HNTs NC gels, NC gels have potential applications in many areas, e.g., biomedical engineering.

Acknowledgments We are grateful for the financial support provided by the National Natural Science Foundation of China with grant number of 51173070, the Key Laboratory of Rubber-plastics (Qingdao University of Science and Technology), Ministry of Education, and the Key Laboratory of High Performance and Functional Polymeric Materials (South China University of Technology), Guangdong province, PR of China.

References

1. Haraguchi K, Takehisa T (2002) Adv Mater 14:1120
2. Haraguchi K (2011) Polym J 43:223
3. Haraguchi K, Takehisa T, Fan S (2002) Macromolecules 35:10162
4. Haraguchi K, Ebato M, Takehisa T (2006) Adv Mater 18:2250
5. Zhu MF, Liu Y, Sun B, Zhang W, Liu XL, Yu H, Zhang Y, Kuckling D, Adler HJP (2006) Macromol Rapid Commun 27:1023
6. Xiong LJ, Hu XB, Liu XX, Tong Z (2008) Polymer 49:5064
7. Haraguchi K, Li HJ, Matsuda K, Takehisa T, Elliott E (2005) Macromolecules 38:3482
8. Haraguchi K, Li HJ (2006) Macromolecules 39:1898
9. Liu Y, Zhu MF, Liu XL, Zhang W, Sun B, Chen Y, Adler HJP (2006) Polym J 47:1
10. Joussein E, Petit S, Churchman J, Theng B, Righi D, Delvaux B (2005) Clay Minerals 40:383
11. Levis SR, Deasy PB (2002) Int J Pharm 243:125
12. Du ML, Guo BC, Jia DM (2010) Polym Int 59:574
13. Lvov YM, Shchukin DG, Mohwald H, Price RR (2008) ACS Nano 2:814
14. Liu M, Guo B, Du M, Jia D (2007) Appl Phys A: Mater Sci Process 88:391
15. Zhou WY, Guo BC, Liu MX, Liao RJ, Rabie ABM, Jia DM (2010) J Biomed Mater Res A 93A:1574
16. Hughes AD, King MR (2010) Langmuir 26:12155
17. Vergaro V, Abdullayev E, Lvov YM, Zeitoun A, Cingolani R, Rinaldi R, Leporatti S (2010) Biomacromolecules 11:820
18. Abdullayev E, Lvov Y (2010) J Mater Chem 20:6681
19. Shchukin DG, Sukhorukov GB, Price RR, Lvov YM (2005) Small 1:510
20. Wagner CD, Riggs WM, Davis LE, Moulder JF, Muilenberg GE (1979) Handbook of X-Ray Photoelectron Spectroscopy. Perkin-Elmer Corporation, Physical Electronics Division, Eden Prairie, Minnesota, USA
21. Podsiadlo P, Kaushik AK, Arruda EM, Waas AM, Shim BS, Xu JD, Nandivada H, Pumplin BG, Lahann J, Ramamoorthy A, Kotov NA (2007) Science 318:80
22. Madejova J (2003) Vib Spectrosc 31:1
23. Simons WW (1978) The Sadtler handbook of infrared spectra. Sadtler Research Laboratories, Informatics Division, Philadelphia, USA
24. Coleman MM, Skrovanek DJ, Hu J, Painter PC (1988) Macromolecules 21:59
25. Guo LH, Sato H, Hashimoto T, Ozaki Y (2010) Macromolecules 43:3897
26. Zhang Y, Tan KL, Liaw BY, Liaw DJ, Kang ET (2000) Thin Solid Films 374:70
27. Misra M, Raja KS (2010) Ordered titanium dioxide nanotubular arrays as photoanodes for hydrogen generation. In: Vayssieres L (ed) On solar hydrogen nanotechnology. John Wiley & Sons (Asia) Pte Ltd, Singapore, pp 265–290

28. Potschke P, Fornes TD, Paul DR (2002) Polymer 43:3247
29. Fu PJ, Xu KL, Song HZ, Chen GM, Yang JP, Niu YH (2010) J Mater Chem 20:3869
30. Krishnamoorti R, Giannelis EP (1997) Macromolecules 30:4097
31. Liu MX, Guo BC, Du ML, Cai XJ, Jia DM (2007) Nanotechnology 18:455703
32. Miyazaki S, Endo H, Karino T, Haraguchi K, Shibayama M (2007) Macromolecules 40:4287
33. Ye YP, Chen HB, Wu JS, Ye L (2007) Polymer 48:6426
34. Rooj S, Das A, Thakur V, Mahaling RN, Bhowmick AK, Heinrich G (2010) Mater Des 31:2151
35. Luca V, Thomson S (2000) J Mater Chem 10:2121
36. Frost RL, Kristof J (1997) Clay Clay Miner 45:551
37. Pasbakhsh P, Ismail H, Ahmad Fauzi MN, Bakar AA (2009) Polym Test 28:548
38. Zhang W, Liu Y, Zhu MF, Zhang Y, Liu XL, Yu H, Jiang YM, Chen YM, Kuckling D, Adler HJP (2006) J Polym Sci A Polym Chem 44:6640